Electronic Supplementary Information for *RSC Advances*

Electronic Supplementary Information

Visible Light-Driven Organic Form-Stable Phase Change Materials for Solar Energy Storage

Yunming Wang, Bingtao Tang* and Shufen Zhang

State Key Laboratory of Fine Chemicals, Dalian University of Technology, P.O. Box 89, West Campus, 2# Linggong Rd, Dalian 116024, China.

Supplementary Methods

Materials synthesis Supplementary Scheme S1 shows the chemical structures and synthetic scheme that was used to obtain visible light-driven organic form-stable phase change material for solar energy storage (VLDOPCM). Throughout the manuscript, the compound 3 is abbreviated as VLDOPCM.

The synthesis was conducted in a two-step polymerization process under an inert atmosphere of nitrogen in flame-dried glassware, as shown in Supporting Information Scheme S1. Firstly, a predetermined amount of dried PEG , toluene-2,4-diisocyanate (TDI) and dibutyltin dilaurate (DBT) in freshly distilled THF were mixed with stirring under nitrogen at 40 °C to 45 °C for 6 h to make an NCO-terminated prepolymer. Then, the stoichiometric amount of the chain extender compound 2 was added, and the reaction was continued at 66 °C for 8 h. The reaction mixture was vacuum-evaporated and further dried at 80 °C for 48 h in vacuum (-0.1 kPa) before testing.

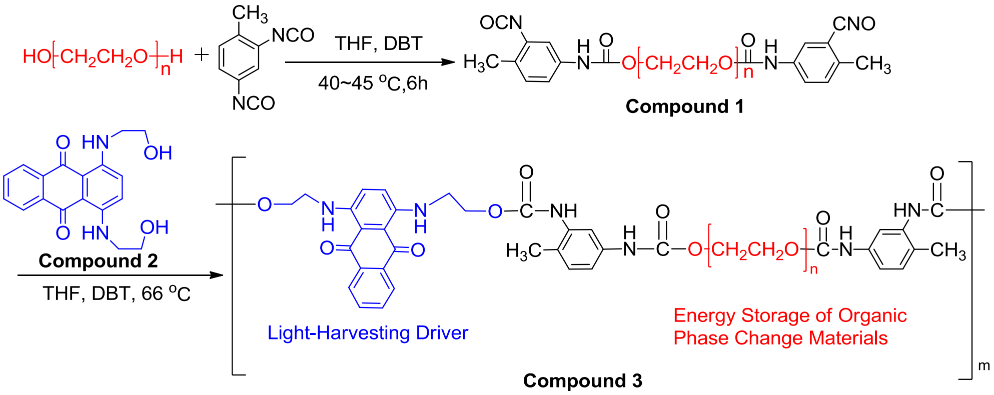

Scheme S1: Chemical structures and synthetic scheme for solar thermal conversion materials with phase change energy storage.

Sunlight irradiation Experimental Section The experimental apparatus can be divided into the following three main components: the light-to-heat conversion system, the data collection and processing devices (Figure S1). The light-to-heat conversion system consists of foam insulation system, the VLDOPCM in a weighing bottle (R=2.5cm) and light source. A power meter (VLP-2000, Changchun Femtosecond Technology Co., Ltd. Jilin, China) was used to measure and verify the power of the light irradiation from solar and simulated light source (CHF-XM-500W, Beijing Chang Tuo Technology Co., Ltd. Beijing, China). The data collecting and processing devices consist of two subsystems, the temperature versus time data collection system and the processing system by computer. The temperature versus time data collection system consists of the Pt thermocouple, the thermocouple-to-analog connector (RS-232-RS-485, Instrument Co., Ltd. Jiangsu Suke, China), and the data logger (SK-130RD106062560021A1, Instrument Co., Ltd. Jiangsu Suke, China).

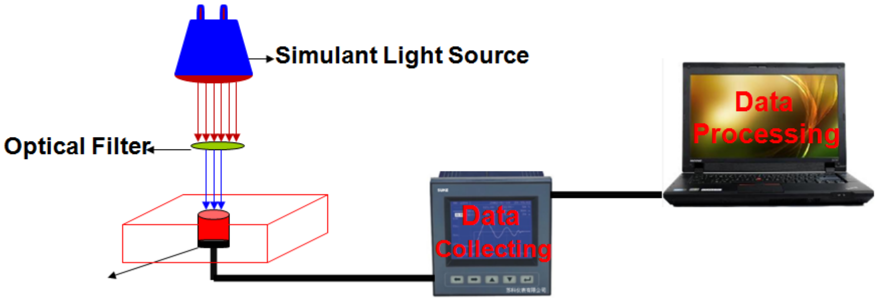

Figure S1: Light-driven transition diagram for the light-to-heat tandem device.

Figure S1 │Schematic showing light-to-heat conversion process in the solar irradiation. Dyes can be used for as an effective photon capture and molecular heater to obtain heat energy into phase change materials. Upon irradiation with the sunlight (P=0.30W, ambient temperature=26.7 °C, Sample=4.0 g), sunlight irradiation experiments for the VLDOPCM and PEG-6000 (control sample) were carried out in 11:41-12:23, 06-9-2011, Dalian, China.

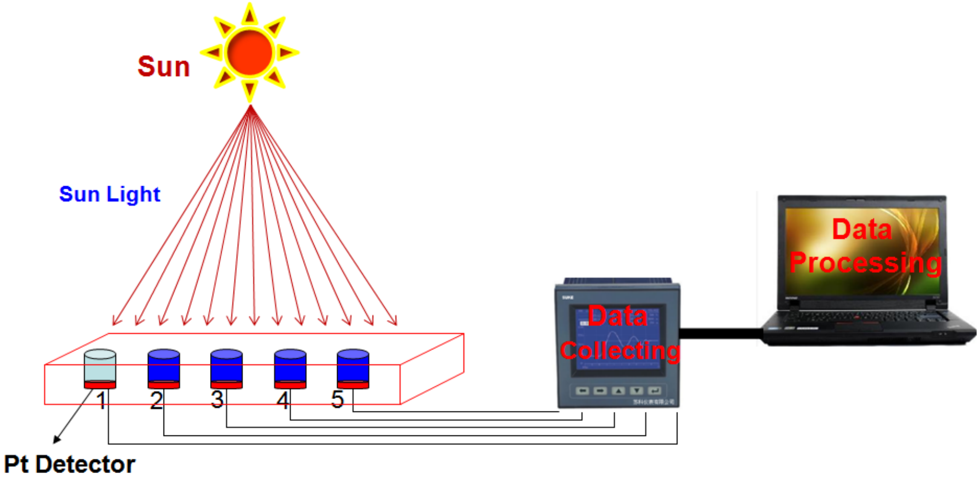

Figure S2: Efficiency diagram for the light-to-heat tandem device.

Figure S2 │Schematic showing Schematic showing the efficiency of photothermal conversion in a simulated light source. The distance between platinum electrode and the sample surface is 1 cm, and the irradiation area is 4.90cm^2.

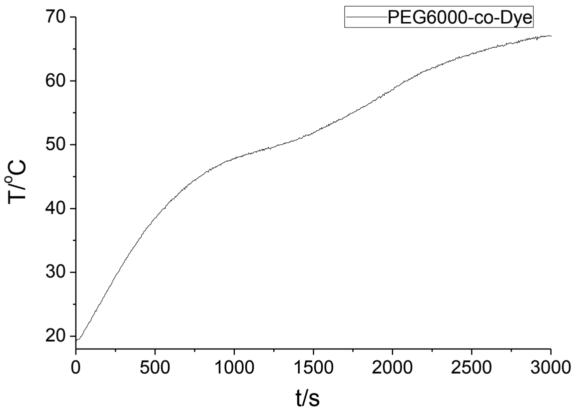

Figure S3: The efficiencies of solar thermal conversion (P=0.33W, λmax=600 nm, ambient temperature=27.0 °C).

Figure S3 │The temperature versus time curve was Light-driven phase transition of organic thermal storage materials under the sunlight irradiation. Using photothermal calculation methods, the developed solar-thermal materials achieved a peak efficiency of 93.7% under 0.33 W irradiation (λ_{max}=600 nm) conditions, which turns out to be remarkably close to 1 according to the Eq. (1). The parameter η is obtained from the following equations (Eq. (1)):

$$\eta = \frac{m\Delta H}{P(T_t - T_f)} \qquad (1)$$

where: η - the efficiencies of light-to-heat conversion,

m-The quality of the VLDOPCM,

ΔH- Transition enthalpy of the VLDOPCM by DSC,

T_t, T_f - the light-driven phase transition temperature of the VLDOPCM before and after phase changing, respectively.

P- the power for the light irradiation of simulated light source.

Eq. (1) │The transduction efficiency of the VLDOPCM was calculated by Eq. (1) under the light irradiation of the simulated light source. We measured the temperature change of the VLDOPCM in foam insulation after simulate light source irradiation at 600 nm. The dyes of the VLDOPCM absorb the light and convert the absorbed energy into heat with a transduction efficiency of η. The crystal state temperature measured is in the interval 48.5 °C < ΔT < 58.7 °C. The mΔH was storing thermal energy of the VLDOPCM harvesting visible light (λmax=600 nm) and converting light to thermal. The $P(T_t-T_f)$ represents the total irradiation energy of the surface of the VLDOPCM. The rate both mΔH and $P(T_t-T_f)$ was the transduction efficiency (η) of the light-to-heat. Using the measured irradiation area of 4.90 cm^2, the visible light power of 0.33W, and the quality of the VLDOPCM, we obtain the transduction efficiency within the interval of η=0.937. The calculated η is remarkably close to 1, as expected for solar energy materials.

UV-visible absorption spectrum Deionized water was redistilled before use. The tetrahydrofuran (THF) was purchased from Guoyao Chemical Company (commercial analytical grade). UV-visible spectra were obtained using a HP-8453 UV/Visible spectrophotometer.

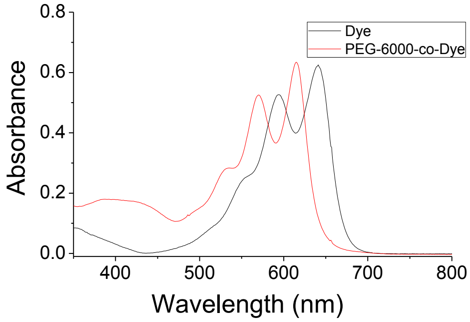

Figure S4: Absorption spectra of the dye intermediate and VLDOPCM in THF solution.

Figure S4 │Absorption curves showing maximum absorption peak of the dye and VLDOPCM in solution.

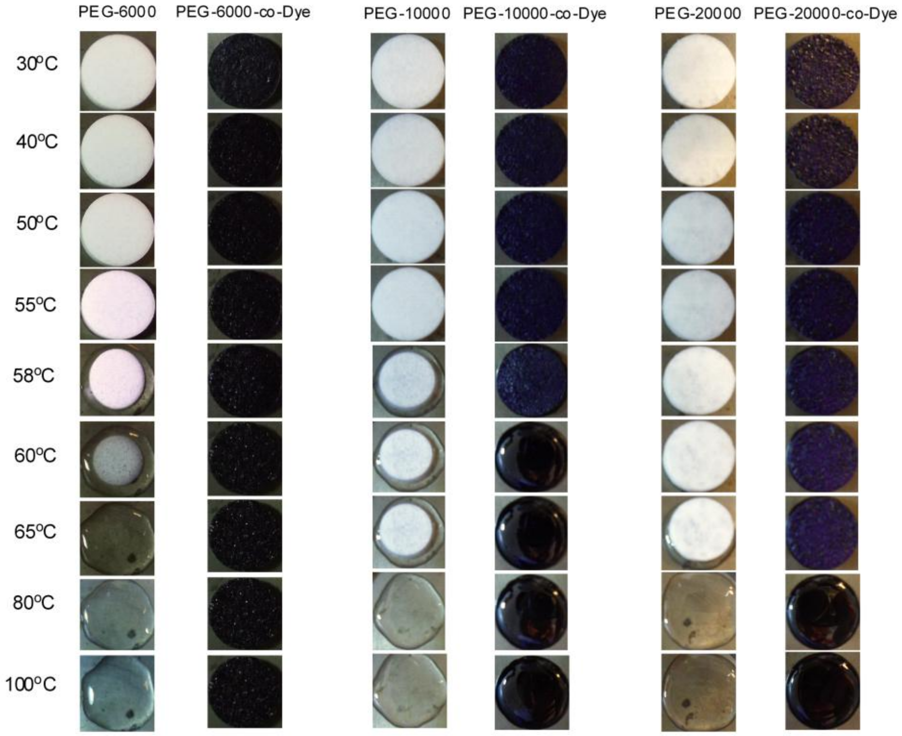

Figure S5: The temperature rise diagram for the VLDOPCMs and pure PEG.

Figure S5 │the photos were shown the states *vs* temperature of the VLDOPCMs and pure PEG. With the rise of the temperature, the pure PEG from solid to liquid, while the VLDOPCM's phase transition remains shape stability and no mobility in the complete heating process, even if the temperature is raised to 80 ºC or higher.

Structural analysis ^{1}H NMR spectra were recorded employing a Varian INOVA 400 NMR spectrometer at 400 MHz, using solutions of the compounds in 0.5 ml of DMSO-d_6 containing TMS (tetramethylsilane) as the internal standard. High resolution mass spectra were recorded on HPLC/Q-Tof MS spectrometer.

Compound 2 ^{1}H NMR, ^{13}C NMR spectra were recorded on a VARIAN INOVA 400 MHz NMR spectrometer. ^{1}H NMR (400 MHz, DMSO-d$_6$, 25 ºC, TMS): δ=3.51-3.54 (m, 4H, CH$_2$), 3.67-3.70 (m, 4H, CH$_2$), 4.96-4.98 (t, 2H, OH), 7.51 (s, 2H, CH), 7.78-7.80 (m, 2H, CH), 8.24-8.26 (m, 2H, CH), 10.95-10.97 (t, 2H, NH); ^{13}C NMR (400 MHz, DMSO-d$_6$, 25 ºC, TMS): δ=59.91, 108.33, 124.72, 125.63,132.20,133.90,146.18,180.48 ppm; MS (ESI, positive) ([M+K]$^+$) (m/z): 349.20.

Compound 3 ^{1}H NMR, ^{13}C NMR spectra were recorded on a VARIAN INOVA 400 MHz NMR spectrometer. ^{1}H NMR (400 MHz, DMSO-d$_6$, 25 ºC, TMS): δ=2.12 (s, 6H, CH$_3$), 3.51 (m, 548H, CH$_2$), 3.63-3.65 (t, 6H, CH$_2$), 3.67-3.69 (t, 4H, CH$_2$), 4.16 (s, 2H, NH), 4.24-4.28 (t, 4H, CH$_2$), 4.77-4.81 (s, 4H, CH$_2$), 6.27-9.25 (m, 12H, Ar-H), 11.03 (s, 1H, NH), 11.36 (s, 1H, NH); ^{13}C NMR (400 MHz, DMSO-d$_6$, 25 ºC, TMS): δ= 17.3, 34.37, 41.10, 43.64, 65.56, 68.93, 71.80, 73.67, 74.11, 75.14, 76.24, 78.47, 81.80, 106.68, 113.41, 116.63, 120.68, 130.73, 138.74, 141.75, 151.93, 152.52, 155.50, 158.72, 159.55, 159.82, 167.62, 188.90 ppm; IR(cm^{-1}) (KBr pellet): 2888 (ν C-H aliphatic), 1727 (ν C=O), 1637 (δ N-H), 1467 (δ CH$_2$), 1281 (ν C-N aromatic), 1241 (ν C-N aliphatic), 1108 (ν_{as} C-O-C exopy), 1060 (ν_s C-O-C ployether).